INELASTIC NEUTRON SCATTERING TECHNIQUES AND ITS APPLICATION TO I_E WATER

Y. WANG and J-C. LI

Originally published as *Physical, Chemical and Biological Properties of Stable Water Clusters,* Proceedings of the First International Symposium. Reprinted here by permission of World Scientific Publishing Company, 1998.

Using inelastic incoherent neutron scattering and Raman scattering techniques, we measured vibrational spectra for the I_E water and compared with high purity normal water (99.96% H_2O). We also tested the I_E water with our crystal growth system which is based on the Bridgman technique. In this paper we report these results.

1. Introduction

Hydrogen bonding is one of the most important and intriguing interactions which dominate our daily lives, and for a long time scientists across different disciplines have endeavored to understand the complex nature of water and of other H-bonded systems. Despite considerable scientific efforts, there are no completely acceptable explanations of most properties of water, often referred to as its 'anomalous' properties.[1-3] The large bond energy and the asymmetrical geometry of the H-bond, combined with the fact that the electrons in the $2s^2p^3$ orbitals of the oxygen atoms can rehybridise in response to the relative configurations of adjacent molecules, giving rise to a large number of abnormal properties of water/ice which cannot be explained by the ordinary rules of physics and chemistry. As a consequence, a large number of models have been proposed in attempts to interpret some of these properties of water, such as the high heat capacity, high melting/boiling temperature and the large density and entropy fluctuations. Meanwhile, a large number of H-bond potentials have also been proposed. Some of these are based on ab initio quantum mechanical calculations[4,5] while others are very arbitrary[6]. Some are good at reproducing the structure of water and others are good at reproducing its thermodynamic properties. No theory can yet provide a coherent explanation of (or complete model for) the water anomalies.

Experimental information about the strength of the H-bond interaction can be obtained by measuring vibrational spectra, because a particular phonon mode (or frequency) will determine the interatomic force constants which, in turn, are the double differentials of the pair-wise potentials. Therefore, measuring dynamic properties constitutes one of the most powerful ways of investigating pair-wise interatomic potentials in a given material. Inelastic incoherent Neutron Scattering (IINS) provides a most suitable probe for studies of vibrational dynamics for given solids. This is because a neutron can simultaneously give insight at the atomic and molecular level about where things 'are' and what they 'do'. Indeed, it is only when this structural and dynamic information is available at the atomic level that it becomes possible to build a complete picture of the behaviour of the world around us. The answers to questions depend on understanding the atomic behaviour of the material. Neutron provides this detailed information about the microscopic behaviour of solids and liquids, and in a major way, has shaped our experimental and theoretical understanding of phenomena ranging from water and

biological systems to chemical surfaces and interfaces.

The advantages of neutron scattering, for the study of molecular dynamics, are due to several remarkable properties of thermal neutrons: for instance, the thermal neutron energy is comparable to the phonon energy and the wavelength associated with the neutron is of the same order as the interatomic distances in the condensed materials. Another characteristic of this probe is that the neutron mass is of the same order as the mass of the scattering nuclei. The scattering is, therefore, sensitive to the structure of the system. In an inelastic scattering experiment, the variation of scattering intensity with neutron energy and momentum transfer is observed. The energy and momentum transfer can be written as:

$$\hbar\omega = E_i - E_f = (\hbar^2/2m)(\mathrm{K}_i - \mathrm{K}_f) \tag{1}$$

$$Q = (\mathrm{K}_i - \mathrm{K}_f) \tag{2}$$

where E (or $\hbar\omega$), **k** and m are the neutron energy, wave-vector and mass, respectively, and i and f refer to the initial and the final conditions of the neutron. Neutron scattering is characterized by the range of $\hbar\omega$ and **Q** in which measurements are carried out. It is interesting to note that for molecular phenomena, the relevant energies are of the order of 10^{-4} to 10^{-1} eV and the wave-vectors are of the order of 10^{-3} - 1Å^{-1} Therefore, neutron scattering appears to be the only probe capable of revealing the scope of the dynamics of molecular solids and liquids on such short space and time scales. In the case of infrared absorption and Raman scattering, the ranges of the energy transfers are essentially the same, but the wavelengths are lengthened by at least three orders of magnitude in comparison with neutron scattering. Moreover, because of the characteristics of the interaction of neutrons with nuclei, there is another unique advantage: giving so called coherent and incoherent scattering. Together, coherent and incoherent scattering provide complete information about the vibrational motions of the atoms or molecules which can be derived from the peak positions, their intensities and their widths. The total neutron scattering cross-sections can be written as sum of the two contributions:

$$\frac{d^2\sigma}{d\omega d\Omega} = \frac{d^2\sigma_{coh}}{d\omega d\Omega} + \frac{d^2\sigma_{inc}}{d\omega d\Omega} \tag{3}$$

$$\frac{d^2\sigma_{coh}}{d\omega d\Omega} = \frac{k_f}{k_i}\exp(-2W)\sum_i \frac{\hbar\sigma_{coh}}{4Nm_i}\sum_{jq}[\mathrm{e}_i(\mathrm{q},j)\cdot\mathrm{Q}]^2 n(\omega)\left[\exp\left(-\frac{\hbar\omega}{2kT}\right)\right] \sum_{\mathrm{n}}\delta(\mathrm{Q}\pm\mathrm{q}\pm 2\pi\mathrm{n})\delta(\omega\pm\omega_i) \tag{4}$$

$$\frac{d^2\sigma_{coh}}{d\omega d\Omega} = \frac{k_f}{k_i}\exp(-2W)\sum_i \frac{\hbar\sigma_{inc}}{4Nm_i}\sum_{jq}[\mathrm{e}_i(\mathrm{q},j)\cdot\mathrm{Q}]^2 n(\omega)\left[\exp\left(-\frac{\hbar\omega}{2kT}\right)\right] [\delta(\omega+\omega_i)+\delta(\omega-\omega_i)] \tag{5}$$

The equations, σ, σ_{inc} and $\sigma_{coh,}$ are the total, incoherent and coherent cross-sections. i labels an atom of mass m_i; $n(\omega)$ is the occupation number at temperature T for the phonon mode of frequency; ω is the phonon frequency in the jth mode for a wave-vector **q** and $\mathbf{e}_j(\mathbf{q}, j)$ is the associated eigen-vector on the ith atom in the unit cell in jth mode. The existence of the second delta function in the double differential of coherent cross-section means that coherent processes are fundamentally different from incoherent processes.

The vibrational spectra of ices have frequently been obtained using IR and Raman techniques. However, because of the proton disorder in most ice structures, the normal selection rules governing the interaction of radiation with the crystal are broken. Hence the analysis of these spectra is difficult. Secondly, the weak intensities associated with the lattice modes (<320 cm^{-1}) provide incomplete information on H-bond interactions and therefore these measurements have been seriously misleading. In contrast, IINS is a more direct probe, because with it all the vibrational modes can be measured with equal sensitivity. The IINS spectrum shows two molecular optic modes at 28 (or 224 cm^{-1}) and 37 meV (or 310 cm^{-1}) rather than one at 220 cm^{-1} as seen in the Raman and IR spectra. Using ice single crystals, these spectra show no dependence on crystal orientation. The spectra of the other forms of proton disordered ices, such as ice V, VI, IX and amorphous ices, show similar features.[7-9] These first direct observations of the two well separated molecular bands is a direct result of the very high flux of neutrons and the excellent energy resolution of the inelastic neutron scattering instruments on ISIS at the Rutherford Appleton Laboratory. The superiority of these measurements has been clearly demonstrated in comparison with earlier neutron data.[10,11]

These results are in direct contradiction to existing dynamical models[11-13] for ice and conventional explanations of the IR and Raman spectra, such as TO and LO splitting.[14] In order to reproduce these INS spectra using lattice dynamic calculations, all available H-bond potentials have been tried. The results of these calculations are far from satisfactory. The two well-separated molecular optic bands in the spectra can only imply that there are two distinct strengths of Hbonds,[15,16] which are related to the two types of proton (or dipole) arrangements in the particular form of ice. Thus, in ice VIII, because of the proton ordering, there is only one type of dipole configuration, which is related to the weak H-bond. Therefore, the higher energy band at 310 cm^{-1} disappears. When the protons in this structure become disordered at high temperature (namely ice VII), the other possible configuration also appears and hence the higher energy optical band reappears. Another interesting phenomenon is that the relative intensities of the strong and weak optical modes are entirely dependent on the relative number (or ratio) of the strong and weak H-bonds in the ice structure. For instance, in ice Ih or ice Ic, the protons are completely disordered, hence the statistics will give one weak H-bond for two strong H-bonds (ratio is 1/3:2/3) which are randomly and isotropically distributed in the ice structure. By partially ordering the structure, we could demonstrate that the relative intensities of the two bands could be altered, which implies that the ratio of the strong and weak dipole arrangements are also changed. Furthermore, the difference of the two H-bond force constants is very large indeed.[15] A simple calculation using the relationship, $\omega = (K/m)^{1/2}$ (where ω is the vibrational frequency and K is the force constant) gives a ratio of the two H-bond force constants as $K^1 : K^2 = (\omega^1 : \omega^2)^2 = 28^2 : 37^2 = 1 : 1.9$ (the exact values determined by the lattice dynamic calculation are 1.1 and 2.1 eV/Å^2). However, the large difference in force constants cannot be produced by the fixed electrostatic interactions (the maximum calculated difference between the strong and weak bonds is <20%).[17] The fundamental source of the splitting of H-bond, therefore, lies at the quantum mechanical level. Based on the above hypothesis, lattice dynamical calculations for ice

Ih were carried out for a large super-lattice, containing 64 molecules (8 unit primary cells), to represent the disordering of protons.[15,16] The results show remarkable agreement not only with the spectrum of phonon density of states, but also with the measured dispersion curves.

This remarkably simple model is capable of reproducing almost every aspect of the measured lattice dynamics of a wide variety of ice structures and indicates the existence of two strengths of H-bonds in the solid phases of water and provides insight into the 'complex' nature of the H-bond. The properties of water are considered abnormal, based on the concept of water as a monodisperse system. However, when we realize that the H-bond interaction is actually bi-functional, all the "abnormal" properties of water become normal. We, therefore, concluded that, if these two types of bond also exist in liquid water, they would provide a mechanism to explain water anomalies, such as the high heat capacity, the high melting/boiling temperatures and the density fluctuations. Because the proportion of the weak/strong H-bonds in water/ice vary by geometric effects and by the laws of thermodynamics, these in turn, will determine the macroscopic properties which can be simulated by Lattice and Molecular Dynamic calculations.

2. Spectroscopic Measurements of the I_E Water

Using similar techniques, we were able to measure vibrational spectra for the I_E water provided by American Technology Group (ATG). These measurements could provide crucial information about the formation mechanism of the I_E clusters which are stable at high temperatures as indicated by Lo et al.[18,19] The IINS measurement was made using TFXA (Time Focused Xtal Analyser) spectrometer on ISIS (a pulsed spallition neutron source) at Rutherford Appleton Laboratory, UK.[20] TFXA is an inverse geometry time-of-flight spectrometer. A "White" energy neutron beam is inelastically scattering by sample, analyzed by graphite crystals (placed at 135° to the direction of the incident neutrons) and beryllium filters, and neutrons with final energy ~4 meV are registered. The measurements give hydrogen bonding vibrational frequencies in the inter- and intra-molecular modes regions up to 500 meV (or ~4100 cm^{-1}). The instrument provides energy resolution, ~1.5% (i.e. *dE/E).* The measured TINS spectra were transferred to the dynamical structure factor $S(Q,\omega)$ vs energy transfer $\hbar\,\omega$ by using a standard data treatment program at TFXA. The background from the empty-can was also measured at similar conditions and was subtracted from the original data. Finally, the measured data was then transferred to the one-phonon spectrum by subtracting the multi-phonon contributions calculated using the iteration technique.[21]

The IINS spectra of both I_E water and normal water at 15K are plotted in Figure 1. The comparison shows that there are no observable differences between the two spectra. This could be due to the fact that the concentrations of I_E clusters in the water used is less than 5% by weight. The IINS signal from the clusters is insignificant. Higher concentrations may be needed in order to see significant difference from the normal ice.

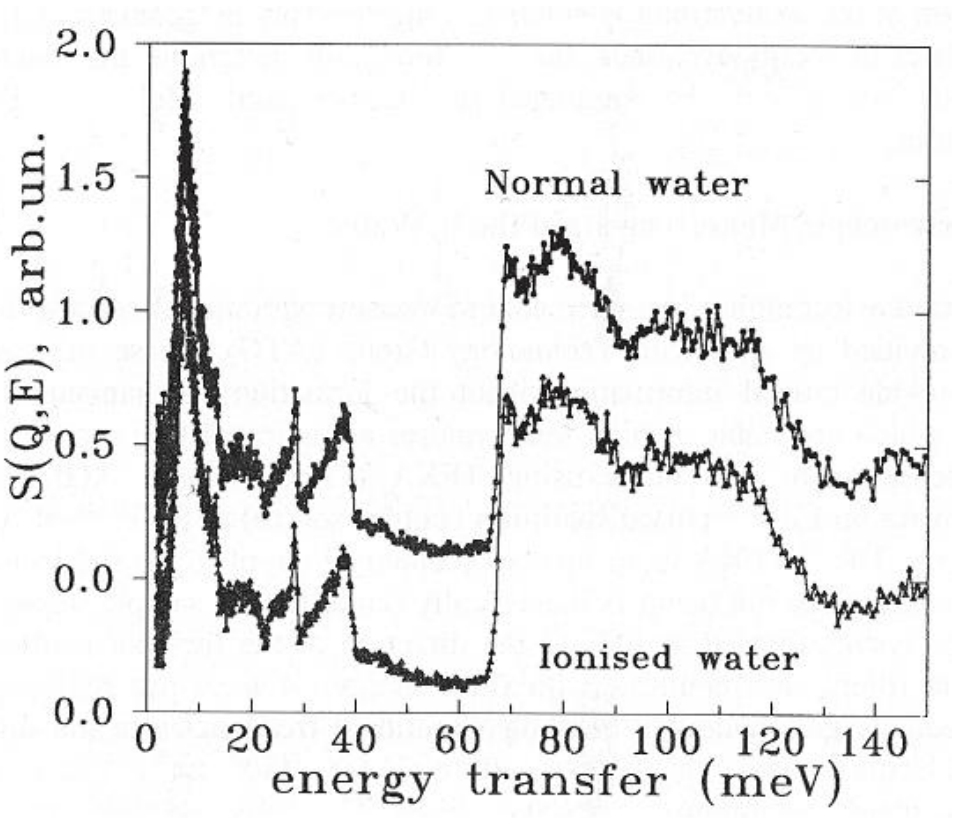

Figure 1. A plot of Inelastic Incoherent Neutron Scattering spectra of the I_E water and normal water measured on TFXA in the energy transfer region below 140 meV at temperature of 15K. The data show that difference between the two spectra is less than the experimental error.

Another series of measurements for the I_E water were made using a standard Raman spectroscopy at 77K. Figure 2 shows the comparison between the I_E water and normal water. We observed that a small peak at energy ~33 meV is stronger in spectrum for the I_E water than that for the normal water and is shifted slightly towards the high energy transfer. More detailed study is needed to understand the source of the feature.

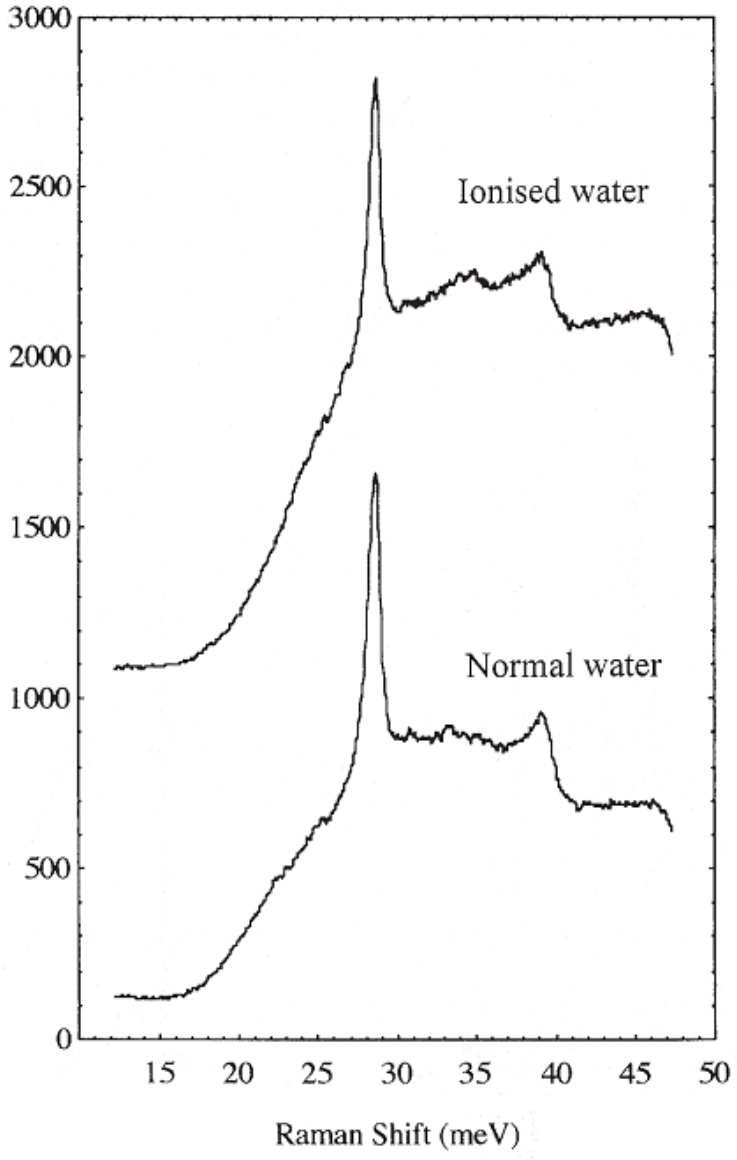

Figure 2. A plot of Raman Scattering spectra of both I_E water and normal water measured at temperature of ~77K. The two spectra are almost identical. There is only a small difference in the molecular optic modes region at energy transfer of ~33 meV.

3. Using the I_E Water for Single Crystal Growth

Apart of spectroscopic studies of the I_E water, we have also attempted to understand the micro-structure of I_E water by growing ice crystals with it. It is our past experience that water which contains impurities inhibits and prevents high quality single crystal growth (i.e. polycrystalline samples can be obtained as the result). This is because ions or other biological materials in water may cause changes in the surroundings and disrupt the growth.

There were two methods of producing ice crystal. One is by fast vaporization of water to cool the water surface down to minus. The crystallization occurs from surface and the single crystal gradually grows downwards.[22] The process takes a few hours. Using this method, we can rapidly

produce single crystals and test the water quality. We found that using this method, we can produce ice crystals from the I_E water provided by ATG as easily as from normal water (99.96% H_2O), although they are less transparent (milking white) than the crystals produced by normal water.

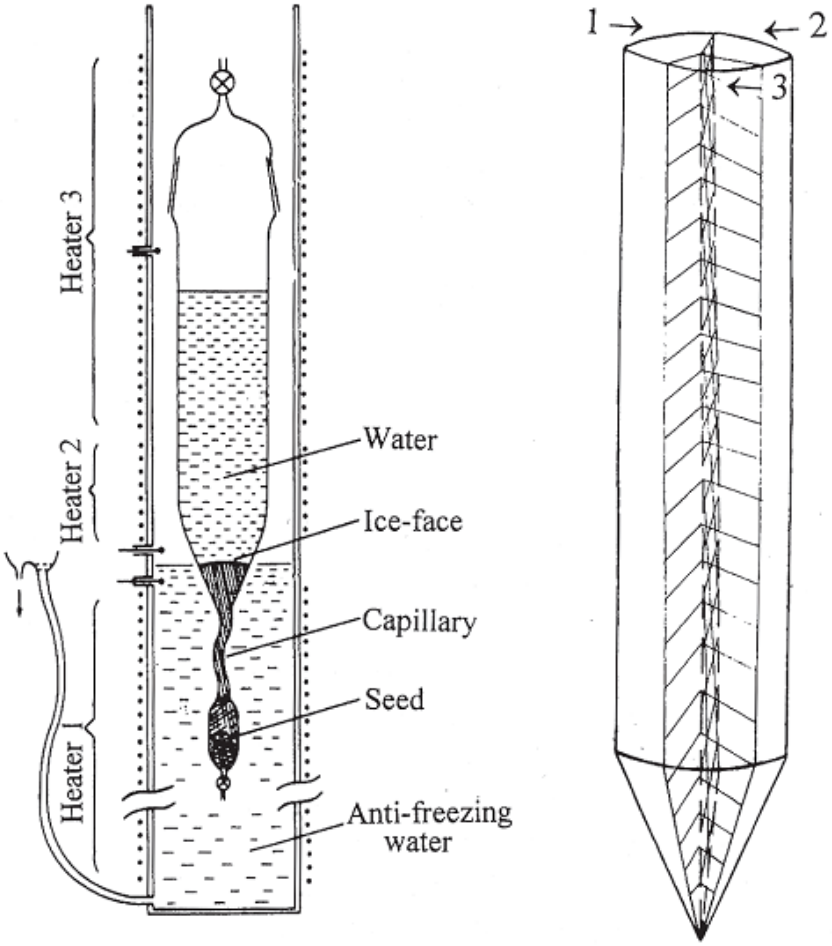

Figure 3. The left diagram shows a schematic illustration of the Bridgman method of crystal growth system[23]. The right diagram is a crystal of ice Ih produced by the system (using the I_E water). In most cases, we were able to produce ice crystals as easily as the high purity normal water. However, for the I_E water labeled with Ds-PB provided by ATG, we obtained 2-3 pieces of single crystals, after a number of attempts as shown in the right diagram.

Another method of producing ice crystal is by the Bridgman method. Figure 3 is schematic illustration of the basic set up for the system[23]. The growth process of ice crystals can be described as follows: Firstly, a growth tube filled with degassed water is dipped into antifreeze at below 8°C in order to form ice nuclei (i.e. seeds). The tube is then suspended inside a larger tube filled with antifreeze liquid at 1.0°C. The temperature above the antifreeze is kept at 0.5°C in order to prevent frozen water. The temperatures are controlled by three independent heaters (Figure 3). Secondly, the growth tube is gradually lowered into the antifreeze liquid in a rate of lcm/day. One of the grains (seeds) will pass the capillary (i.e. a process of elimination) and a single crystal is grown while the tube is lowered. This system allows us to produce high quality ice crystals, with a very low concentration of dislocations, for neutron scattering experiments.

After several attempts with this system, we found that the I_E water gives as good a quality of single crystals, in most cases, as normal water with 99.96% H_2O. However, there are occasionally two or three column crystals produced along the length of the growth tube when we use the I_E water labeled with Ds-PB (see the right diagram in Figure 3). This may not be due to the I_E water itself, but the conditions surrounding the growth tube.

References

1. H.S. Frank *WATER: A Comprehensive Treatise, VI*, ed. F. Franks, (Plenum Press 1972).
2. D. Eisenberg and W. Kauzmann, *The Structure and Properties of Water* (Oxford University Press, Oxford 1965).
3. P.V. Hobbs *Ice Physics* (Clarendon Press, Oxford 1974).
4. H. Kistenmacher *et al, J. Chem. Phys.* **60**, 4455 (1972).
5. C. Lee, *et al, Phys. Rev. Lett.* **69**, 462 (1992).
6. M.D. Morse and S.A. Rice, *J. Chem. Phys.* **76**, 650 (1982).
7. J-C. Li *et al, J.Phys.: Condens. Matter* **4**, 2109 (1992).
8. J-C. Li *et al, Chem. Phys. Lett.* **241**, 290 (1995).
9. J-C. Li and D.K. Ross, *J. Condens Matt.* **6**, 10823 (1994).
10. H. Prask *et al, J. Chem. Phys.* **48**, 3367 (1968).
11. B. Renker, in *Physics and Chemistry of Ice,* ed. E. Whalley *et al*, (University of Toronto Press, Toronto 1973).
12. P. Bosi *et al, J. Chem. Phys.* **59**, 4578 (1973).
13. D.D. Klug and E. Whalley, *J.Glaciol,* **21**, 55(1978), and comment, *J. Chem. Phys.* **71**, 1513 (1979).
14. T.T. Wong and E. Whalley, *J. Chem. Phys.* **65**, 829 (1976).
15. J-C. Li and D.K. Ross, *Nature*, **365**, 327 (1993).
16. J-C. Li, *J. Chem. Phys.* **105**, 6733 (1996).
17. J-C. Li, *J. Phys. Chem. B,* **101**, 6237 (1997).
18. S.Y. Lo, *et al, Modern Phys.Lett. B,* **10**, 921(1996).
19. S.Y. Lo, *Modern Phys. Lett. B,* **10**, 909 (1996).
20. S.F. Parker *et al, The TFXA User-Guide*, Rutherford Appleton Laboratory: Technical Report No.RAL-TR-95-036 (1995).
21. A.I. Kolesnikov *et al, J. Phys.: Condens. Matter*, **6**, 375 (1994).
22. N.N. Khusnatdinov and V.F. Petrenko, *J. Crystal Growth*, **163**, 420 (1996).
23. M. Ohtomo *et al, J. Physique*, **48**, C1595 (1987).